Correlation Between Mesh Geometry and Stiffness Matrix Conditioning for Nonlocal Diffusion Models

Jibum Kim*

Department of Computer Science and Engineering, Incheon National University, Incheon, 406-772, South Korea.

Received 27 January 2014; Accepted (in revised version) 28 September 2014

Available online 5 November 2014

Abstract. Nonlocal diffusion models involve integral equations that account for nonlocal interactions and do not explicitly employ differential operators in the space variables. Due to the nonlocality, they might look different from classical partial differential equation (PDE) models, but their local limit reduces to partial differential equations. The effect of mesh element anisotropy, mesh refinement and kernel functions on the conditioning of the stiffness matrix for a nonlocal diffusion model on 2D geometric domains is considered, and the results compared with those obtained from typical local PDE models. Numerical experiments show that the condition number is bounded by $c\delta^{-2}$ (where c is a constant) for an integrable kernel function, and is not affected by the choice of the basis function. In contrast to local PDE models, mesh anisotropy and refinement affect the condition number very little.

1. Introductions

Nonlocal diffusion equations and nonlocal peridynamic models have received considerable attention in recent years. Peridynamic theory was developed by Silling [1]. Nonlocal diffusion and peridynamic theory involve integral equations rather than differential equations to model cracked surfaces and deformations, and have also been extensively applied elsewhere — e.g. to turbulence [2], porous flow [3], nanofibers [4, 5], and fracture and damage modelling of membranes [4]. Refs. [6, 7] provide recent surveys of nonlocal diffusion and peridynamic models, and their applications. It has been shown that a nonlocal peridynamic model reduces to a classical local model (such as in elasticity theory) when the length scale (horizon) goes to zero [8]. The effect of various kernel functions on the nonlocal advection problem has been investigated for a 1D problem [9]. Researchers have also studied finite difference and finite element discretisation of nonlocal diffusion and

---

*Corresponding author. *Email address:* jibumkim@incheon.ac.kr (J. Kim)

peridynamic models [10–13], including *a posteriori* error analysis and the connection between the horizon and the condition number in Ref. [10]. Condition number estimates and upper bounds for the discretised linear system, and the effect of the horizon and mesh size on the condition number for isotropic elements, have been investigated [14]. Interactions between mesh geometry, mesh refinement and the condition number of the global stiffness matrix for classical PDE have also been considered. Thus the connection between the anisotropy of mesh elements and the condition number for elliptic PDE was investigated in Ref. [15]; various mesh quality metrics, interpolation error and the condition number for elliptic, parabolic and hyperbolic PDE were explored in Ref. [16]; and connections between the mesh quality metric, preconditioner and the linear solver for elliptic PDE were studied computationally in Refs. [17, 18].

In this article, the Galerkin finite element method is used to discretise a linear nonlocal diffusion system, in order to study the effect of the anisotropy of the mesh element (element shape), mesh refinement (element size) and kernel functions on the condition number for a nonlocal diffusion model on 2D geometric domains. There are various nonlocal models, such as a bond-based model [1, 13] and a state-based model [19]. We consider a bond-based nonlocal model that involves central forces between particles [1, 13, 20], and numerically demonstrate the effect of an integrable kernel function on the condition number for both piecewise linear and piecewise constant basis functions. Conditioning is important, because it affects the accuracy of the solution and the convergence rate in solving the discretised linear system [15, 16]. This article is the first to explore the connections between anisotropy, mesh refinement and the condition number for 2D meshes with various kernel functions for a scalar nonlocal diffusion model. This is computationally challenging for various reasons. First, two different quadrature rules are needed to approximate the double integral terms on 2D geometric domains, to avoid the singularity of the denominator when the condition number of the global stiffness matrix is computed. Second, it is desirable to compute approximately the area of intersection between the horizon (δ) and the triangular element when the quadrature rule is used. Finally, the number of intersections between the horizon and the triangular element increases significantly as the level of mesh refinement increases, and so is computationally expensive.

The conditioning of the stiffness matrix is investigated for both piecewise constant and piecewise linear basis functions, assuming an integrable kernel function. In each case, the effect of changing the anisotropy and mesh size (h) on the conditioning of the scalar nonlocal diffusion model is examined. The analytical results show that the condition number is bounded by $c\delta^{-2}$ (where c is a constant) when a finite integrable kernel function is employed [14]. For an integrable kernel function, it is shown numerically in each case that the condition number is barely affected by the choice of basis function. The constant c in the condition number bound ($c\delta^{-2}$) is computed for uniform triangular and rectangular meshes in 2D. For general elliptic PDE, it is well-known that the condition number is proportional to h^{-2} when the mesh has the same anisotropy on uniform triangular and rectangular meshes in 2D [16]. Mesh anisotropy also affects the condition number for general elliptic PDE — e.g. if θ is the smallest angle in the right triangle, then the condition number is proportional to $\sin^{-1}(2\theta)$ [15] such that the condition number sharply increases

as θ approaches 0. The effect of the anisotropy and mesh size on the condition number is investigated, and the difference between the nonlocal diffusion model and the related classical PDE model is also discussed.

This article is organised as follows. In Section 2, the nonlocal diffusion model is described, and in Section 3 the quadrature rules and basis functions employed are discussed. The condition number of the global stiffness matrix is considered in Section 4, and results from numerical experiments on 2D rectangular meshes are presented in Section 5. Conclusions and plans for future work are in Section 6.

2. A Scalar Nonlocal Diffusion Model

The nonlocal diffusion model considered replaces a PDE with an integral equation, on assuming that a solid body consists of small particles that interact with each other [20]. The interaction between particles is called a *bond*, and each particle interacts with other particles within a spherical surface of radius δ (the horizon). The internal force applied to particle at any point $v = (x, y)$ is denoted by

$$Lu(v) = \int_H f\left(u\left(v'\right) - u(v)\right) dv', \tag{2.1}$$

where L is a linear integral operator, u is a displacement vector, H is a spherical neighbourhood of particles which interact with a particle x, f is a pairwise peridynamic force, and dv' is an infinitesimal volume related with a particle v'. From Newton's Second Law,

$$\rho\ddot{u}(v) = Lu(v) + b(v), \tag{2.2}$$

where ρ is the mass density, and $b(v)$ is an external force. Combining (2.1) and (2.2) results in

$$\rho\ddot{u}(v) = \int_H f\left(u\left(v'\right) - u(v)\right) dv' + b(v). \tag{2.3}$$

If ξ denotes the distance between v and v', then f is 0 if ξ is larger than δ (the notion of nonlocality). The horizon (δ) and force (f) between v and v' over the geometric domain Ω are illustrated in Fig. 1. For a microelastic material, commonly considered in the nonlocal literature and also assumed here, the interaction between two particles is modelled by an elastic spring [1, 13]. For the bond-based nonlocal model with a microelastic material, (2.3) can be reduced to the linearised model described by

$$\rho\ddot{u}(v) = \int_H c\frac{\left(v' - v\right) \otimes \left(v' - v\right)}{|v' - v|^p}\left(u\left(v'\right) - u(v)\right) dv' + b(v), \tag{2.4}$$

where $\otimes$ is the Kronecker product. Refs. [1, 13] provide further information on the properties of microelastic models. A steady state is assumed here such that $\ddot{u}(v) = 0$, when (2.4) reduces to

$$\int_H c\frac{\left(v' - v\right) \otimes \left(v' - v\right)}{|v' - v|^p}(u\left(v'\right) - u(v)) dv' + b(v) = 0. \tag{2.5}$$
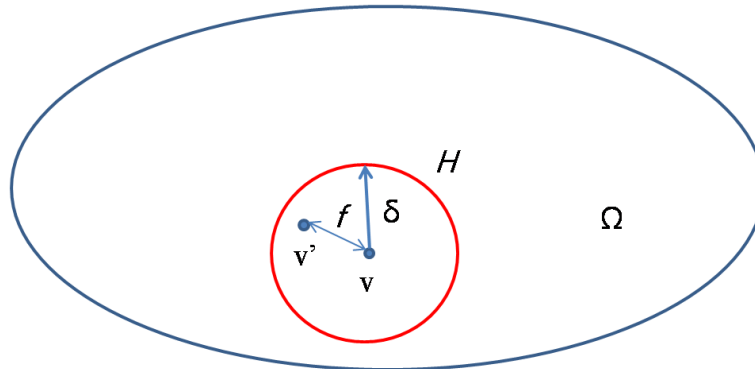
Figure 1: The horizon (δ) and the force (f) between v and v' inside the neighbourhood H, within the domain Ω. (The point v does not interact with any points beyond the distance δ.)

For a one-dimensional domain (e.g. $v = x$) with a Dirichlet boundary condition, (2.5) becomes

$$\frac{1}{\delta^{4-p}} \int_{v-\delta}^{v+\delta} \frac{u(v) - u(v')}{|v-v'|^p} \, dv' = b(v), \; v \in \Omega, \tag{2.6}$$

where $u(v) = g(v)$ on the boundary $\partial\Omega$, and the global stiffness matrix A may be computed using a standard Galerkin finite element method with basis functions $\phi(v)$ further discussed in Section 3. The $M \times M$ matrix A, where M respectively denotes the number of mesh elements for a piecewise constant basis function or the number of vertices for a piecewise linear basis function, is

$$A_{ij} = \frac{1}{\delta^{4-p}} \left(\int_H \frac{\phi_j(v) - \phi_j(v')}{|v-v'|^p}, \phi_i(v) \right) \tag{2.7}$$

involving an inner product — i.e. more explicitly, we have the double integral form

$$A_{ij} = \frac{1}{\delta^{4-p}} \int_I \phi_i(v) \int_H \frac{\phi_j(v) - \phi_j(v')}{|v-v'|^p} \, dv' \, dv, \tag{2.8}$$

in which I represents all neighbourhoods of the point v where $\phi_i(v)$ is nonzero and $1/|v-v'|^p$ is called the kernel function. The matrix A is symmetric, positive-definite and sparse [13]. Fig. 2 shows an example of the sparsity pattern of the global stiffness matrix (2.8) on a 2D geometric domain.

Compared with the corresponding PDE model sparsity pattern, more nonzero values arise due to the nonlocality. The sparsity band of the global stiffness matrix is determined by the horizon length δ and mesh size h. Another important difference between classical PDE and nonlocal diffusion models is the definition of the boundary condition. Fig. 3 shows the difference between the classical PDE boundary condition and the nonlocal diffusion boundary condition. For classical PDE, the boundary condition on $\partial\Omega$ is defined for boundary points — whereas in nonlocal diffusion models the boundary conditions refer to a boundary area $B\Omega$, so additional mesh generation is required on the boundary area $B\Omega$ to the horizon δ.
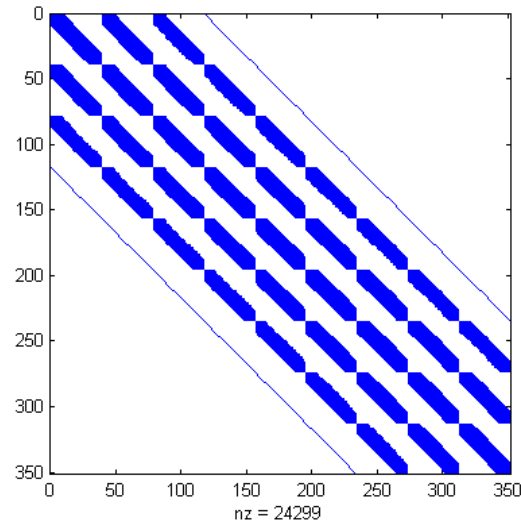
Figure 2: One example of the sparsity pattern of the matrix A for the nonlocal diffusion model, where nz is the number of nonzero values in A.

(a) Classical PDE boundary condition

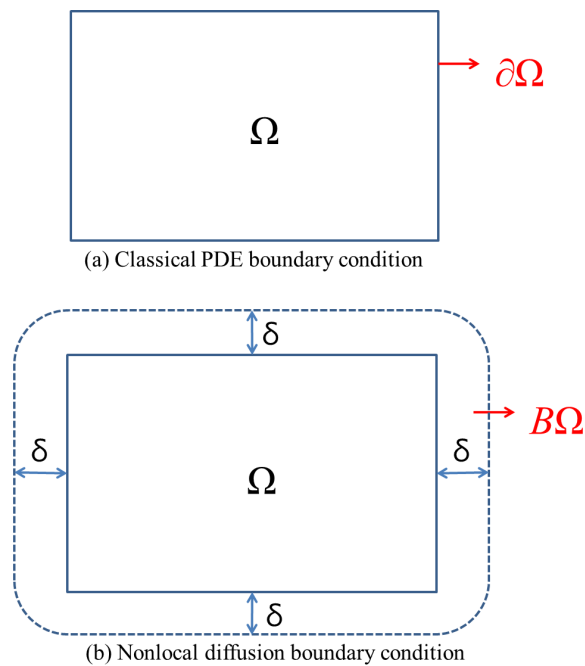(b) Nonlocal diffusion boundary condition

Figure 3: Boundary conditions for (a) a classical PDE model and (b) a nonlocal diffusion model. For classical PDE problems, the boundary condition is only specified on the boundary points, whereas for nonlocal diffusion models all mesh elements belonging to $B\Omega$ correspond to the boundary condition.

3. Quadrature Rules and Basis Functions

3.1. Quadrature rules for a triangle

It is computationally inexpensive to compute (2.8) using quadrature rules similar to [13]. In particular, one may choose two different quadrature rules for inner and outer integrals,
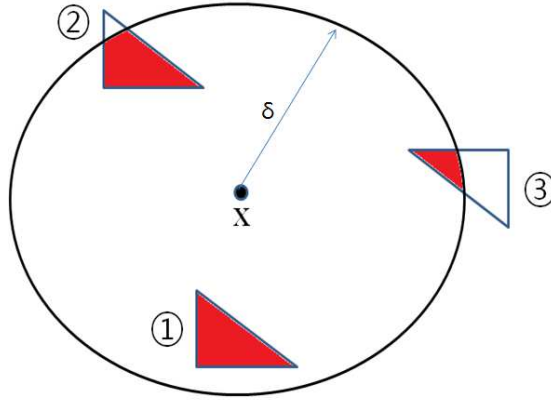
Figure 4: Three different cases for computing $|T|$, involving the intersection of T with δ. (Only intersection areas inside the horizon are computed.)

because the denominator term $|v - v'|$ could otherwise be singular. The quadrature rule for the integration of f over a triangle is

$$\int_T f(x, y) \, dx \, dy \approx |T| \sum_{i=1}^{m} f(x_i, y_i) w_i, \tag{3.1}$$

where T is a triangle in Ω, $|T|$ is the area of T and m is the number of points used in the associated quadrature rule [21]. One-point and three-point quadrature rules are used to approximate the outer and inner integrals, respectively. For the unit triangle with vertices $\{(0, 0), (0, 1), (1, 0)\}$, the one-point quadrature rule (centroid) with degree of precision 1 is

$$\begin{cases} (x_1, y_1) = (1/3, 1/3), \\ \qquad w_1 = 1. \end{cases} \tag{3.2}$$

For the unit triangle with vertices $\{(0, 0), (0, 1), (1, 0)\}$, the three-point quadrature rule with degree of precision 3 is [21]

$$\begin{cases} (x_1, y_1) = (2/3, 1/6), \; (x_2, y_2) = (1/6, 2/3), \; (x_3, y_3) = (1/6, 1/6), \\ \qquad w_1 = 1/3, \; w_2 = 1/3, \; w_3 = 1/3. \end{cases} \tag{3.3}$$

Since the horizon is a circle and the mesh element is a triangle, another approximation is used to compute the intersection area of T with the horizon (circle). Three different cases are considered where the intersection of T with δ is computed. In the first case, the entire triangle is inside the horizon, when $|T|$ is the area of a triangle — cf. case 1 in Fig. 4. When only part of a triangle is located inside the horizon as shown in cases 2 and 3 in Fig. 4, the exact intersection area is expensive to compute, so approximations are used to compute the intersection areas of T with δ.

3.2. Basis functions

It has been reported that the stiffness matrix conditioning for nonlocal diffusion problems is less affected by the choice of the basis functions than by the mesh size [10]. Both piecewise constant and piecewise linear basis functions are considered here, to investigate the effect of mesh geometry on stiffness matrix conditioning for nonlocal diffusion models, and whether the choice of basis functions is important. (Previously, the interactions between the mesh anisotropy, basis functions and the stiffness matrix conditioning have not been investigated.)

Continuous piecewise constant (PC) basis functions cannot be used for classical PDE models because the derivative of zero is not defined, but they can be used for nonlocal diffusion models since they involve integral equations. The PC basis function is 1 if x is on the jth element, but otherwise it is 0. The continuous PC basis functions used are

$$\phi_j(x,y) = \begin{cases} 1, & \text{if } (x,y) \in T_j, \\ 0, & \text{otherwise}. \end{cases} \tag{3.4}$$

As in a popular approach to the numerical solution of classical PDE models, standard "hat" functions are used for continuous piecewise linear (PL) basis functions, and only function values for points inside the support of the basis function need be computed. The continuous PL basis function with respect to the jth vertex is

$$\phi_j(x,y) = \begin{cases} -\dfrac{[(y_l-y_k)(x-x_k)+(x_k-x_l)(y-y_k)]}{[(x_j-x_k)(y_j-y_l)-(x_j-x_l)(y_j-y_k)]}, & \text{if } (x,y) \in \text{neighbourhood of } j^{th} \text{ vertex}, \\ \qquad\qquad 0, & \text{otherwise}, \end{cases} \tag{3.5}$$

where k and l are two other vertices of a triangular element to which (x,y) belongs.

4. Condition Number of the Global Stiffness Matrix

4.1. A nonlocal diffusion model

The connection between the horizon, mesh size, and condition number of the global stiffness matrix is studied analytically for an integrable kernel function [14]. The condition number is bounded as follows:

$$\text{cond}(A) \leq c \min\left\{\delta^{-2}, h^{-2}\right\},$$

where c is a constant and h is the mesh size (here the diagonal length of right triangles). Since many nonlocal problems assume that δ is greater than h, the condition number of the global stiffness matrix is bounded by the horizon δ — i.e. the condition number is proportional to δ^{-2} when δ is greater than h, indicatomg that decreasing the horizon increases the upper bound of the condition number.

Two different choices of basis and kernel functions in (2.8) are considered. The power of a kernel function p is such that in d-dimensional space (where $d \in \{1, 2, 3\}$),

$$\int_H \frac{1}{|v - v'|^p} \, dx \begin{cases} = \infty, & p \geq d, \\ < \infty, & p < d, \end{cases} \tag{4.1}$$

and the case $d=2$ is considered here. If the power of a kernel function $p \geq 2$, (2.8) is not integrable (infinite), but otherwise (if $p < 2$) it is integrable (finite).
For the integrable kernel function, p in (4.1) is set to 1.

1. **Piecewise constant basis function with an integrable kernel function.**
   For this kernel function, the condition number is bounded — i.e.

   $$\text{cond}(A) \leq c \min\left\{\delta^{-2}, h^{-2}\right\} \tag{4.2}$$

   where c is a constant, or

   $$\text{cond}(A) \leq c\,\delta^{-2} \tag{4.3}$$

   when δ is taken to be larger than the mesh size h.

2. **Piecewise linear basis function with an integrable kernel function.**
   Similarly, the condition number is bounded — i.e.

   $$\text{cond}(A) \leq c\,\delta^{-2}, \tag{4.4}$$

   when δ is larger than the mesh size h.

Consequently, the condition number converges to a stable level for the mesh refinement and anisotropy in each case.

4.2. General second-order elliptic PDE

The effect of the mesh size and mesh anisotropy on the conditioning of the global stiffness matrix has been studied for general second-order elliptic PDE models [15]. Suppose a general second-order elliptic PDE model is to be solved on a uniform structured triangular mesh with right triangles in a 2D rectangular domain. Let θ be the smallest angle in the right triangle, when the condition number is proportional to $\sin^{-1}(2\theta)$ [15], so the condition number sharply increases and approaches infinity as θ approaches 0. If the mesh elements are assumed to have the same anisotropy, the condition number is proportional to h^{-2}.

The mathematical relationship between the mesh element shape, mesh size, and the condition numbers of the stiffness matrix for second-order elliptic PDE was investigated in Ref. [16]. The Galerkin formulation of the finite element method results in the global stiffness matrix K. If λ_{max} and λ_{min} respectively denote the largest and smallest eigenvalues of the global stiffness matrix (K) for the isotropic second-order elliptic PDE, then

$$\text{cond}(K) = \lambda_{max}/\lambda_{min}. \tag{4.5}$$

For the second-order elliptic PDE with isotropic PDE coefficients considered, λ_{min} is proportional to the area of the smallest element on the mesh, while λ_{max} is highly related with the mesh element shape. It was also reported that λ_{max} increases as the anisotropy of the mesh element increases. In particular, for 2D geometric domains with triangular elements λ_{max} is approximately bounded by

$$\lambda_{max} \leq \frac{l_1^2 + l_2^2 + l_3^2}{4A}, \tag{4.6}$$

where l_1, l_2, and l_3 are three edge lengths of the triangle and A is the area of the triangle.

5. Numerical Results on 2D Rectangular Meshes

The effect of mesh element anisotropy, mesh refinement and various kernel functions on the condition number of the global stiffness matrix A in (2.8) was investigated on 2D structured rectangular meshes — i.e. $\Omega = (0, 1) \times (0, 1)$. The mesh size h is the diagonal length of each right triangle, and θ and $2/\pi - \theta$ were the two acute angles of each triangle. The 2-norm condition number was used to compute the condition number of the global stiffness matrix A — and an OpenMP library with C sped up the computation for computing the condition number with the code parallelised, leaving the condition number unaffected. The machine employed had a 48 core AMD opteron 2.3 GHz processor with 8GB of RAM.

Structured triangular meshes on the rectangular geometric domain were considered, as shown in Fig. 5. Additional triangular elements were generated in the area surrounding Ω, inside the area where the boundary conditions are defined. One example of the anisotropic mesh, where the aspect ratio is 4, is shown in Fig 6. The total number of elements was fixed for both isotropic and anisotropic meshes, for given mesh refinements and δ. The aspect ratio of a right triangle is defined by

$$aspect\ ratio = W/w, \tag{5.1}$$

where w and W are the shortest and second shortest edge lengths, respectively. Fig. 7 shows the definition of the aspect ratio of a triangle.

5.1. Case 1: Piecewise constant basis function with an integrable kernel function

For the piecewise constant basis functions, the power of the kernel function p in (2.8) was 1 for an integrable kernel function. Table 1 shows the condition number of the global stiffness matrix A, for various mesh sizes and horizons (δ) and both isotropic and anisotropic meshes. When δ is small (viz. $\delta = 0.2$), a large portion of the triangular elements within the horizon intersects the horizon (cf. cases 2 and 3 in Fig. 4), and the increased ratio of intersections between the horizon and the triangular elements decreases the numerical stability.

Table 1: Condition number of the global stiffness matrix A for piecewise constant basis functions with an integrable basis kernel function ($p=1$). The number of mesh elements is the number of elements in Ω.

(a) Isotropic meshes with aspect ratio 1

Isotropic mesh	δ=0.2	δ=0.3	δ=0.4
200 elements (no mesh refinement)	16.33	8.70	5.65
800 elements (1 level of mesh refinement)	17.47	9.06	5.79
3,200 elements (2 levels of mesh refinement)	18.09	9.10	5.83
12,800 elements (3 levels of mesh refinement)	18.40	9.13	5.89

(b) Anisotropic meshes with aspect ratio 4

Anisotropic mesh	δ=0.2	δ=0.3	δ=0.4
200 elements (no mesh refinement)	15.98	8.00	5.53
800 elements (1 level of mesh refinement)	17.55	8.95	5.70
3,200 elements (2 levels of mesh refinement)	17.88	8.29	5.86
12,800 elements (3 levels of mesh refinement)	18.24	8.77	5.92
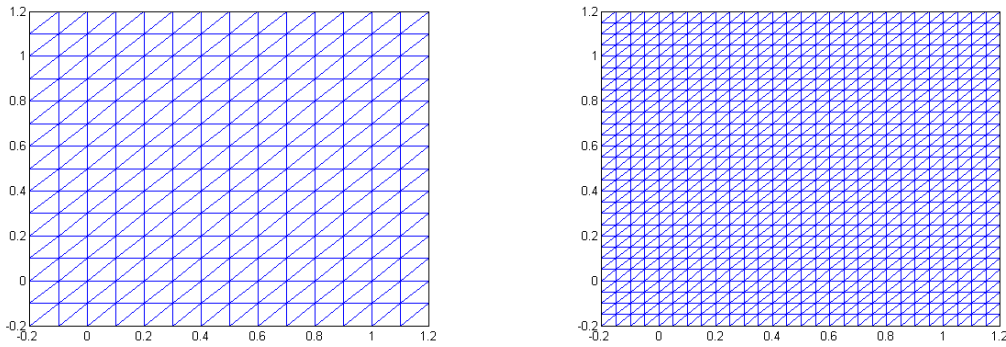
(a) Isotropic mesh with no mesh refinement ($\delta = 0.2$)

(b) Refined isotropic mesh with one level of mesh refinement ($\delta = 0.2$)

Figure 5: (a) Initial isotropic mesh; (b) refined mesh with one level of mesh refinement.

1. **Number of elements (level of mesh refinement) and δ fixed, but the anisotropy of the elements varied.** Figs. 8 and 9 show the connection between δ, anisotropy and the condition number. It is observed that increasing anisotropy of the elements does not affect the condition number, and that the condition number of the global stiffness matrix A is proportional to δ^{-2} when δ is larger than h. The condition number is bounded by $c\delta^{-2}$, where c is a constant close to 1.

2. **Anisotropy of the elements and δ fixed, but the level of mesh refinement varied.** Figs. 10 and 11 show the connection between the horizon (δ), mesh refinement and the condition number of the global stiffness matrix. Similar to the previous numer-
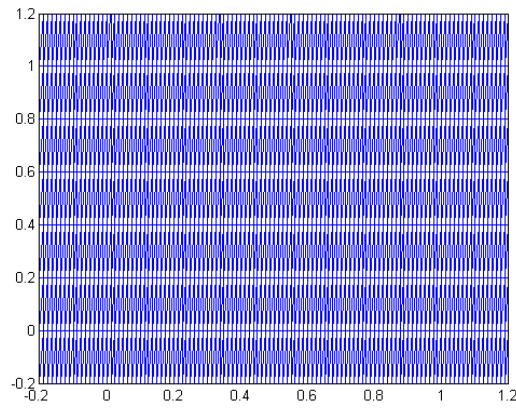
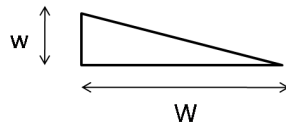Figure 6: Anisotropic mesh (aspect ratio = 4, $\delta = 0.2$).

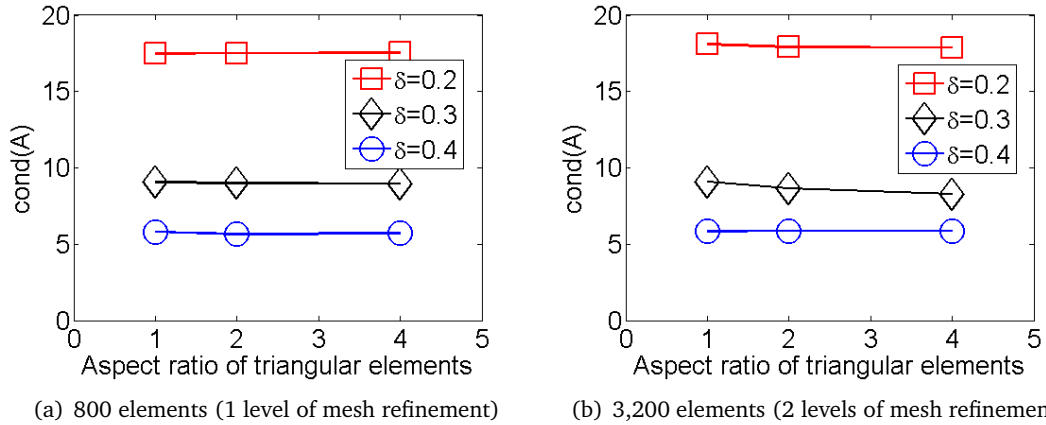Figure 7: The aspect ratio of a triangle, defined as W/w [22].

(a) 800 elements (1 level of mesh refinement) (b) 3,200 elements (2 levels of mesh refinement)

Figure 8: Case 1: Condition number of the global stiffness matrix A for a fixed level of mesh refinement, and the anisotropy of the elements and δ varied.

ical results, the condition number of the global stiffness matrix A is proportional to δ^{-2} when δ is larger than h. The condition number of the global stiffness matrix A converges to a stable level as the number of mesh refinement levels increases, and it is bounded by $c\delta^{-2}$ where c is a constant close to 1.
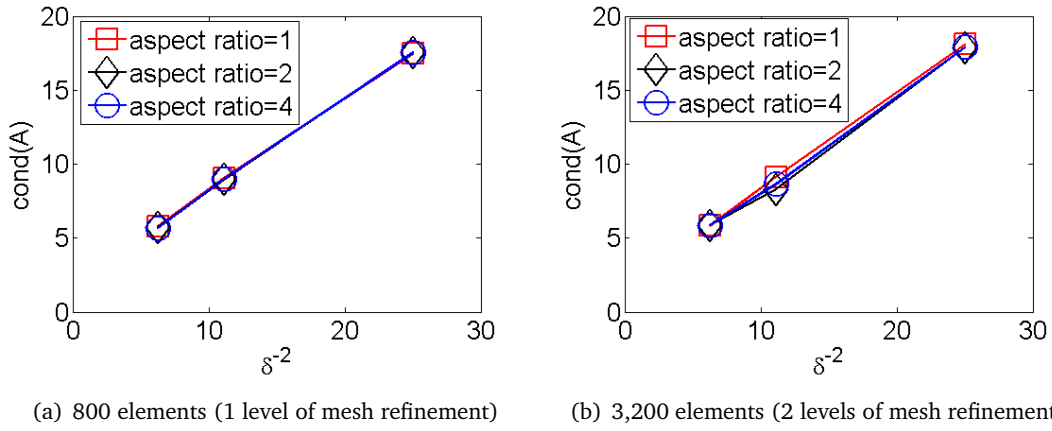
(a) 800 elements (1 level of mesh refinement)   (b) 3,200 elements (2 levels of mesh refinement)

Figure 9: Case 1: Condition number of the global stiffness matrix A as a function of δ^{-2} for a fixed number of elements (mesh refinement), and the anisotropy of the elements and δ varied.
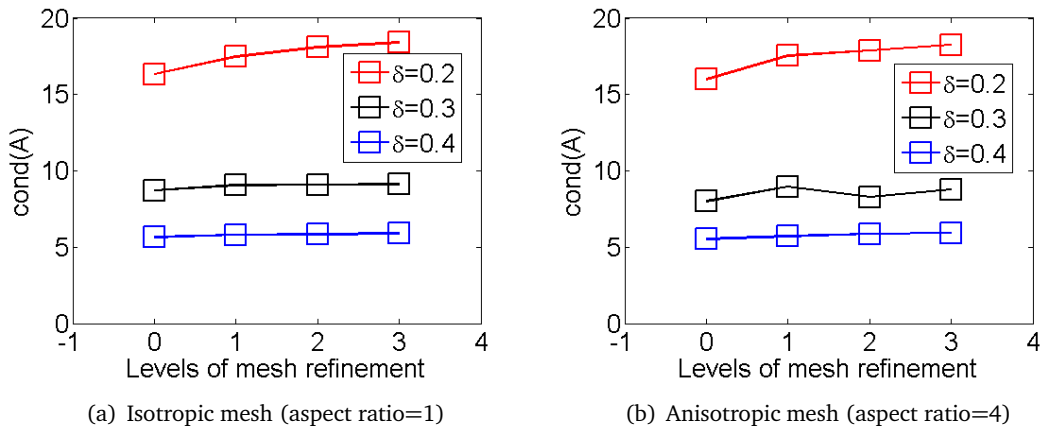

(a) Isotropic mesh (aspect ratio=1)   (b) Anisotropic mesh (aspect ratio=4)

Figure 10: Case 1: Condition number of the global stiffness matrix A for fixed anisotropy, and the level of mesh refinement and δ varied.

5.2. Case 2: Piecewise linear basis function with an integrable kernel function

For the piecewise linear basis functions, the power of the kernel function p in (2.8) was 1 for an integrable kernel function. Based on the analytical results in Section 4, the overall trend was expected to be similar to that seen for piecewise constant basis functions with an integrable kernel function. However, since hat basis functions were used, the condition numbers are not exactly same. Table 2 shows the condition number of the global stiffness matrix for various mesh sizes and horizons (δ), for both isotropic and anisotropic meshes.

1. **Fix the level of mesh refinement and δ, and vary the anisotropy of the elements.**
   Figs. 12 and 13 show the connection between the horizon (δ), anisotropy, and the condition number of the global stiffness matrix. Similar to the case of the piecewise constant basis function with integrable function, the condition number of the global
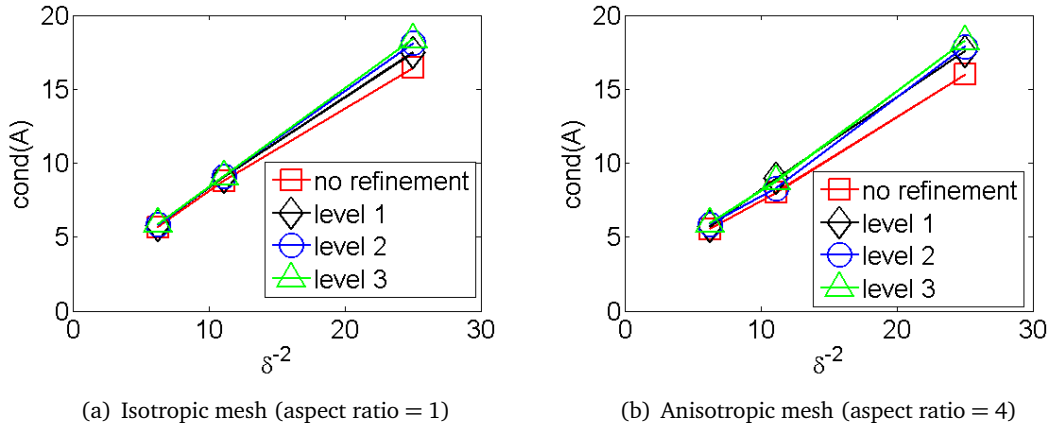
(a) Isotropic mesh (aspect ratio = 1)   (b) Anisotropic mesh (aspect ratio = 4)

Figure 11: Case 1: Condition number of the global stiffness matrix A as a function of δ^{-2} for fixed anisotropy, and the level of mesh refinement and δ varied. (Here, "level" means the level of mesh refinement.)

Table 2: Condition number of the global stiffness matrix A for piecewise linear basis functions with an integrable basis kernel function ($p = 1$). The total number of elements changes with respect to the horizon δ. (The number of mesh elements is the number of elements in Ω.)

(a) Isotropic meshes with aspect ratio 1

Isotropic mesh	δ=0.2	δ=0.3	δ=0.4
200 elements (no mesh refinement)	10.28	6.12	4.00
800 elements (1 level of mesh refinement)	13.35	7.20	4.70
3,200 elements (2 levels of mesh refinement)	15.31	7.85	4.98
12,800 elements (3 levels of mesh refinement)	16.08	8.16	5.08

(b) Anisotropic meshes with aspect ratio 4

Anisotropic mesh	δ=0.2	δ=0.3	δ=0.4
200 elements (no mesh mesh refinement)	11.69	7.36	4.31
800 elements (1 level of mesh refinement)	14.43	7.46	4.89
3200 elements (2 levels of mesh refinement)	15.78	8.17	5.18
12800 elements (3 levels of mesh refinement)	16.73	8.58	5.33

stiffness matrix A is proportional to δ^{-2}. Also, the condition number is bounded by a constant number even if the aspect ratio of the triangular elements is increased. These results are consistent with the analytical results in Section 4. The condition number is seen to be bounded by δ^{-2}.

2. **Fix the anisotropy of the elements and δ, and vary the level of mesh refinement.** Figs. 14 and 15 show the connection between the horizon (δ), mesh refinement, and the condition number. We also observe that the condition number is proportional to δ^{-2} and is bounded by $c\delta^{-2}$. We also observe that the condition number of the global

(a) 800 elements (1 level of mesh refinement)   (b) 3,200 elements (2 levels of mesh refinement)
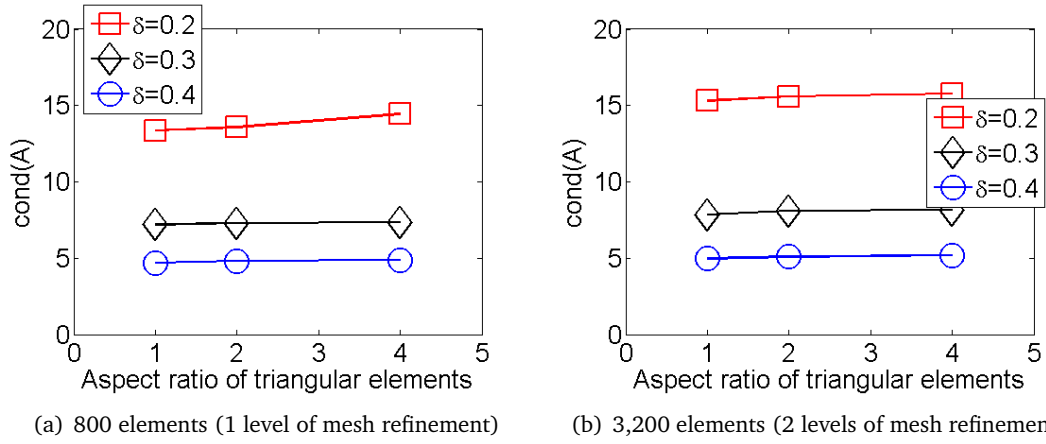
Figure 12: Case 2: Condition number of the global stiffness matrix A for a fixed level of mesh refinement (number of elements), but the anisotropy of the elements and δ varied.
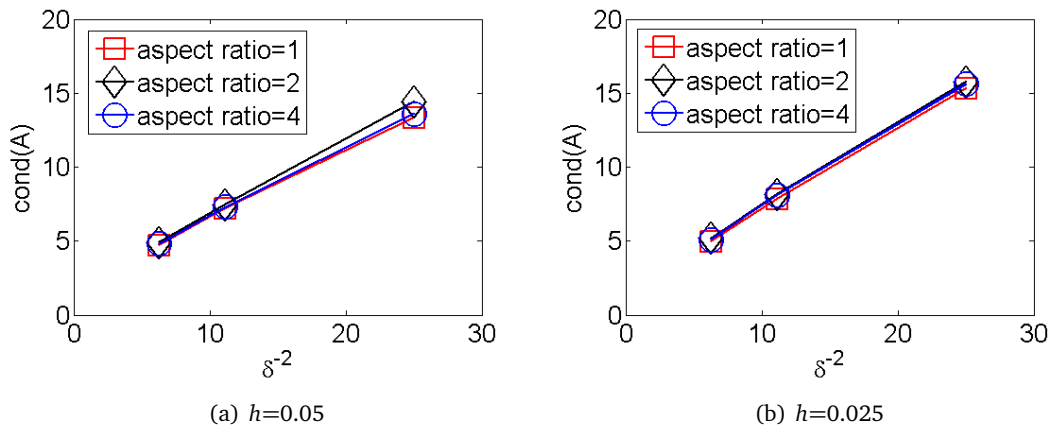

(a) $h=0.05$ (b) $h=0.025$

Figure 13: Case 2: Condition number of the global stiffness matrix A for a fixed level of mesh refinement, but the anisotropy of the elements and δ varied.

stiffness matrix A converges to a stable level as the number of mesh refinement levels increases. Numerical results show that c is close to 1.

6. Conclusions

The effects of anisotropy, mesh refinement and various kernel functions on the condition number for a 2D nonlocal diffusion model have been investigated. This is the first study to examine the connections between the anisotropy and the conditioning on 2D geometric domains with a scalar nonlocal diffusion model. The Galerkin finite element method is used to discretise the nonlocal diffusion model and investigate the effects of various choices of basis functions on the condition number of the global stiffness matrix. Numerical results
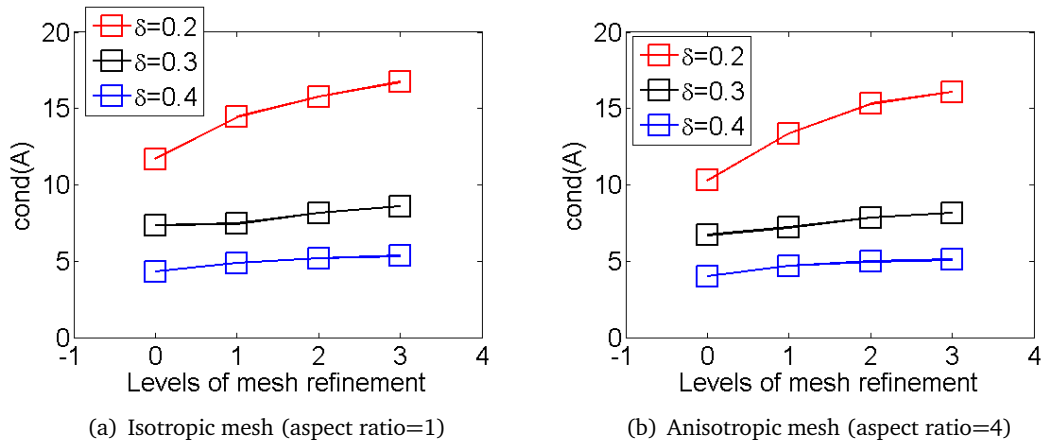
(a) Isotropic mesh (aspect ratio=1)   (b) Anisotropic mesh (aspect ratio=4)

Figure 14: Case 2: Condition number of the global stiffness matrix A for fixed anisotropy, but the level of mesh refinement and δ varied.

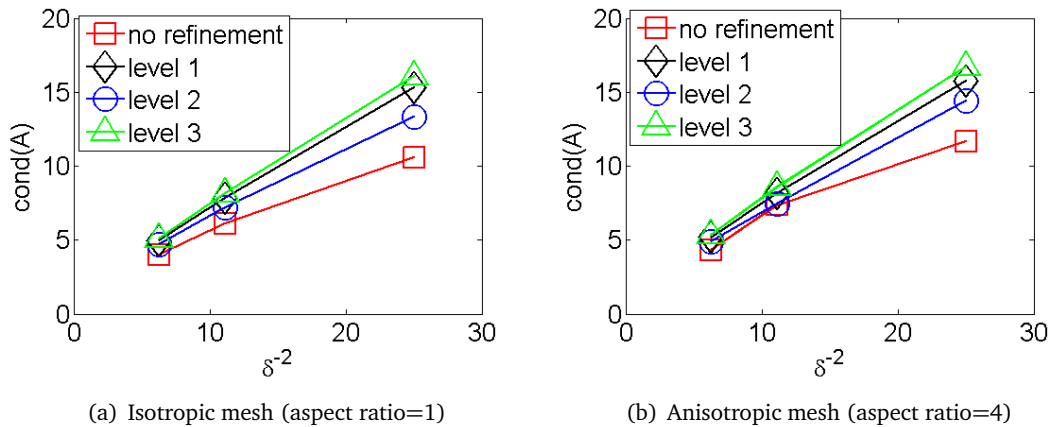(a) Isotropic mesh (aspect ratio=1)   (b) Anisotropic mesh (aspect ratio=4)

Figure 15: Case 2: Condition number of the global stiffness matrix A for fixed anisotropy and varying the level of mesh refinement and δ. (Here, "level" means the level of mesh refinement.)

consistent with the analytical results were obtained when an integrable kernel function is employed. In respect of the integrable kernel function, the condition number is bounded by $c\delta^{-2}$ (where c is a constant) and is unaffected by the choice of the basis functions when δ is larger than the mesh size h. The numerical results show that the constant c is close to 1 on 2D uniform triangular and rectangular domains for an integrable kernel function. Unlike elliptic PDE calculations, the mesh anisotropy and mesh refinement affect the condition number very little.

For future research, other nonlocal diffusion models on unstructured geometric domains may be considered. The sparsity pattern of a nonlocal diffusion model differs from that of PDE model, since the sparsity pattern is affected by the horizon radius. A preconditioner to decrease the condition number for a 2D nonlocal diffusion model could also be developed.

Acknowledgments

References

[1] S.A. Silling, *Reformulation of elasticity theory for discontinuities and long-range forces*, J. Mech. Phys. Solids **48**, 175-209 (2000).

[2] O.G. Bakunin, *Turbulence and Diffusion: Scaling versus Equations*, Springer Series in Synergetics, Springer (2008).

[3] G. Dagan, *The significance of heterogeneity of evolving scales to transport in porous formations*, Water Resources Res. **30**, 3327-3336 (1994).

[4] F. Bobaru, S.A. Silling and H. Jiang, *Peridynamic fracture and damage modeling of membranes and nanofiber networks*, in Proc. XI International Conference Fract., Turin, pp. 5748:1-6 (2005).

[5] F. Bobaru, *Influence of van der Waals forces on increasing the strength and toughness in dynamic fracture of nanofiber networks: A peridynamic approach*, Model. Simul. Mater. Sc. **15**, 397-417 (2007).

[6] E. Emmrich, R.B. Lehoucq and D. Puhst, *Peridynamics: A nonlocal continuum theory*, in *Meshfree Methods for Partial Differential Equations* VI (2012).

[7] S.A. Silling and R.B. Lehoucq, *Peridynamic theory of solid mechanics*, Adv. Appl. Mech. **44**, 73-168 (2010).

[8] S.A. Silling and R.B Lehoucq, *Convergence of peridynamics to classical elasticity theory*, J. Elasticity **93**, 13-37 (2008).

[9] Q. Du, J.R. Kamm, R. B. Lehoucq and M.L. Parks. *An approach to nonlocal, nonlinear advection*, Technical report 2011-3164J, Sandia National Laboratories (2011).

[10] B. Aksoylu and M. Parks, *Variational theory and domain decomposition for nonlocal problems*, Appl. Math. Comput. **217**, 6498-6515 (2011).

[11] R.W. Macek and S.A. Silling, *Peridynamics via finite element analysis*, Finite Elem. Anal. Des. **43**, 1169-1178 (2007).

[12] S.A. Silling and E. Askari, *A meshfree method based on the peridynamic model of solid mechanics*, Comput. Struct. **83**, Advances in Meshfree Methods, 1526-1535 (2005).

[13] X. Chen and M. Gunzburger, *Continuous and discontinuous finite element methods for a peridynamic model of mechanics*, Comput. Methods Appl. Mech. Eng. **200**, 1237-1250 (2010).

[14] K. Zhou and Q. Du, *Mathematical and numerical analysis of linear peridynamic models with nonlocal boundary conditions*, SIAM J. Numer. Anal. **48**, 1759-1780 (2010).

[15] Q. Du, D. Wang and L. Zhu, *On mesh geometry and stiffness matrix conditioning for general finite element spaces*, SIAM J. Numer. Anal. **47**, 1421-1444 (2009).

[16] J. Shewchuk, *What is a Good Linear Finite Element? Interpolation, Conditioning, Anisotropy and Quality Measures*, Technical Report, Department of Computer Science, University of California, Berkeley (2003).

[17] J. Kim, S.P. Sastry and S.M. Shontz, *Efficient solution of elliptic partial differential equations via effective combination of mesh quality metrics, preconditioners, and sparse linear solvers*, Proc. 19th International Meshing Roundtable Conference, pp. 103-120, Chattanooga (2010).

[18] J. Kim, S.P. Sastry and S.M. Shontz, *A numerical investigation on the interplay among geometry, meshes, and linear algebra in the finite element solution of elliptic PDE*, Eng. Comput. **28**, 431-450 (2012).

[19] S. Silling, M. Epton, O. Weckner, J. Xu and E. Askari, *Peridynamic states and constitutive modeling*, J. Elast. **88**, 151-184 (2007).

[20] Y. Kebing, X.J. Xin and K.B. Lease, *A new method of adaptive integration with error control for bond-based peridynamics*, in Proc. of the World Congress on Engineering and Computer Science, San Francisco (2010).

[21] J. Burkardt, *Quadrature rules for triangles*, http://people.sc.fsu.edu/~jburkardt.

[22] M. Picasso, *Adaptive finite elements with large aspect ratio based on an anisotropic error estimator involving first order derivatives*, Comput. Method Appl. Math. **196**, 14-23 (2006).